International Conference on Advances in Manufacturing and Materials Engineering, AMME 2014

Optical interferometric properties of iridescent nanoporous anodic alumina

Suresh D. Kulkarni[a], K.S. Choudhari[a]*, C. Santhosh[a]

[a]Department of Atomic and Molecular Physics, Manipal University, Manipal-576 104, India

Abstract

Highly ordered nanoporous anodic alumina (NAA) membranes with varying pore properties were fabricated using two step electrochemical oxidation of aluminum. A study on optical reflective interferometric properties of NAA was conducted. The influence of pore properties including pore diameters, interpore distance and pore lengths on the reflection spectra was explored. Variation of reflection intensities with different angles of incidence showed the iridescence of NAA membranes. Such NAA nanostructures are promising for the use as substrates for various biomedical sensing applications.

*Keywords:*nanoporous anodic alumina; scanning electron microscopy; optical interferometric properties.

* Corresponding author. Tel.: +91824 2925073
E-mail address: choudhari.k@ gmail.com

1. Introduction

Nanoporous anodic alumina (NAA) membrane has emerged as a versatile and inexpensive template, in recent years, for fabricating a whole host of nanostructures which exhibit fascinating electronic and optical properties [Li et al., 1998; Choudhari et al., 2013; Kumeria et al., 2014]. Highly ordered and well organized NAA membranes possess homogeneous morphology of parallel nanopores which grow normal to the substrate's surface and have a very narrow distribution of pore sizes and interpore spacing displaying closely packed honeycomb like structure. Owing to the exceptional properties such as extremely high pore density and high aspect ratio a wide range of

materials can be grown using NAA templates by several physical and chemical methods such as pulsed laser deposition, sputtering [Gao et al., 2009; Sudheendra et al., 2012a; Sudheendra et al., 2012b], electrodeposition [Biswas et al., 2007; Liu et al., 2008], chemical vapor deposition [Sklar et al., 2005] etc. NAA membranes are used as templates for synthesis of nanomaterials such as nanodots, nanowires, nanorods and nanotubes of different materials including various metals, semiconductors and conducting polymers [Belwalkar et al., 2008; Choudhari et al., 2012b].Recently it has been reported that, NAA membranes can be used for color production applications similar to the structural colors observed in nature such as those in insects and bird feathers which have many useful characteristics including high reflectivity, polarization and iridescence properties [Xu et al., 2012]. It has also been observed that precise tuning of whole light range can be achieved by varying pore lengths of NAA membranes along with the deposition of metal nanolayers [Wang et al., 2011]. Kumeria et al. have recently reported about the structural engineering of NAA and their real-time and label-free biosensing applications and drug release monitoring using the optical reflection spectra [Kumeria et al., 2014; Kumeria et al., 2013].

A profound knowledge of the physical properties of NAA membranes is crucial to spread further the NAA membrane application areas. The structural and thermal properties of NAA are reported previously [Choudhari et al., 2012b]. Herein, in this study, we report on the optical interferometric properties of NAA membranes fabricated with various pore dimensions. NAA membranes with highly ordered nanopore arrays were prepared with varying pore properties. We investigated the use of optical reflective spectrum to characterize the NAA membrane thickness. In addition, the relationship between effective optical thickness and fringe patterns and change in color intensity with angle of incidence are discussed.

2. Experimental

The NAA membranes were prepared by a two-step electrochemical anodization, as per our earlier reports [Choudhari et al., 2012a; 2012b]. In brief, high purity aluminum foils (Merck, thickness 0.3 mm) were cleaned in acetone for 1 hour followed by 20 minutes of ultrasonic degreasing, before carrying out the anodization. The samples were then annealed at 500 °C for 5 hours. Next, the samples were rinsed with double distilled water and then etched in 2 M sodium hydroxide to remove the natural oxide present on the substrate. The samples were then dipped in 1.5 M nitric acid for 3 minutes. The samples were electrochemically polished at a current density of 200 mA/cm^2 in a mixture of concentrated chromic and phosphoric acid solutions (in the ratio 2:8) for 8 minutes, rinsed in running double distilled water and dried in the warm air stream. Anodization was carried out in 0.3 M oxalic acid and 10 wt% phosphoric acid solutions at various anodization voltages. The temperature of the solution was maintained at 5°C. A two-electrode configuration was used with the electropolished substrate as the anode and a cleaned aluminum sheet, of the same area as that of the anode, as the cathode. First stage anodization was performed for 2 hours. The formed alumina layer was removed by immersing the specimen in a mixture of 1.8 wt% chromic acid and 6 wt% phosphoric acid at 60°C for 2 hours. Subsequent step of second stage anodization was carried out with the same initial conditions for various durations to obtain NAA of different thicknesses.

The NAA samples were characterized by field-emission scanning electron microscope, Carl Zeiss Ultra 55 FESEM (Carl Zeiss, Jena, Germany). Atomic force microscopy imaging was carried out using Agilent 5500 AFM (Agilent Technologies, Palo Alto, CA, USA). UV-VIS-NIR diffuse reflectance spectra were recorded on a Perkin Elmer Lambda 950 UV/Vis/NIR spectrophotometer equipped with an integrating sphere (Perkin Elmer, Waltham, MA, USA). The reflectance data were collected in the spectral range 300 to 2300 nm from the NAA membranes. Effective optical thickness ($2n_{eff}L$, where n_{eff} is the effective refractive index and L is the thickness of the NAA membranes) was obtained by calculating the slope of a straight line that was fitted on the graph of integer (m) vs. $1/\lambda$ (where λ is wavelength) in Matlab.

3. Results and Discussions

Before starting anodization the aluminum substrates were electropolished in order to reduce the roughness of the surface. After electropolishing the substrate's surfaces appear smooth and mirror-like shiny [Choudhari et al., 2012b]. During first stage of anodization the pores nucleate randomly and hence the pores are irregular on the surface. After removing this alumina using wet etching the surface is left with concave dimples throughout the aluminum substrate [Choudhari et al., 2012a]. This nanopatterned substrate is anodized again with the same initial

conditions. Fig. 1 shows an SEM and an AFM image of NAA prepared by two stage anodization in 0.3 M oxalic acid at 40 V. It can be seen that the pores are well ordered and close-packed hexagonally patterned in a honeycomb-like structure. It is well known that the best periodic arrangement can be observed for alumina prepared at 40 V compared to any other nearby voltages and that the pore properties of NAA depend on the applied anodization potential [Choudhari et al., 2012b]. The ordered pores of NAA have a very narrow distribution of pore sizes around 45 nm and an interpore distance of approximately 100 nm. The detailed analysis of pore properties of NAA prepared at different voltages and with different pore widening durations are given elsewhere [Choudhari et al., 2012b; 2013].
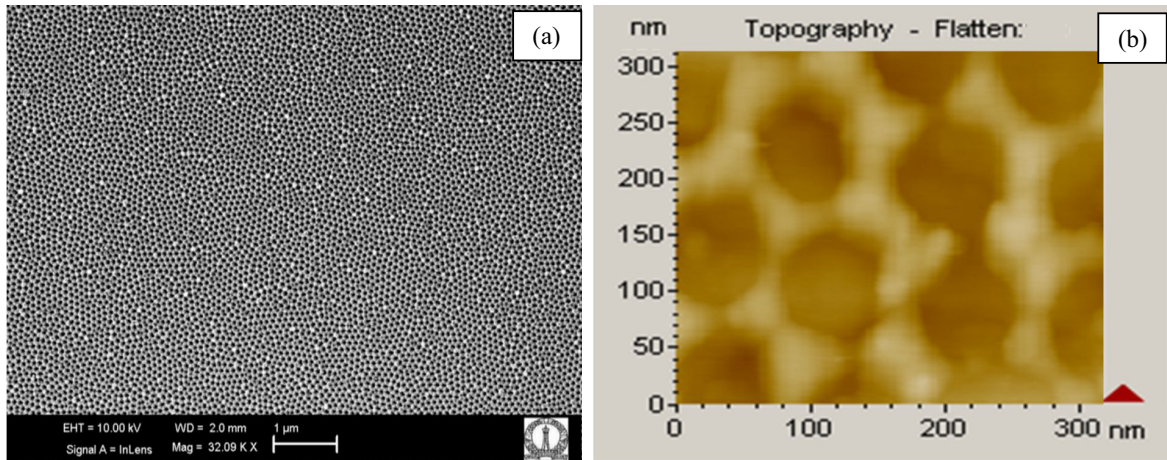

Fig. 1. Microscopic images of NAA prepared in oxalic acid at 40 V. (a) FESEM image and (b) AFM image

By controlling the anodization voltage from 40 to 150 V, we fabricated NAA with a range of pore diameters from 45 to 225 nm and interpore distance from 100 nm to 395 nm. Fig. 2(a) and (b) shows the linear dependence of pore diameters and interpore distances with the applied voltage which is in agreement with our previous reports [Choudhari et al., 2012b; 2013]. From these data, rate of pore diameter growth was observed to be about 1.6 nm/V and the interpore distance growth rate was around 2.7 nm/V in accordance with the available literature values [Li et al., 1998]. The thickness or the length of the nanopores of NAA thin films depends on the duration of anodization and the applied voltage. The growth rate of NAA pores is different for different voltages for a given time period. Fig. 2(c) shows the dependence of nanopore growth on anodization time under a constant anodization voltage (40 V). Average growth rate for pores was found to be 36 nm/min at this voltage. At higher anodization voltages the growth rate increases and in those cases also the pore length exhibits linear dependence on anodization time at a given applied voltage value.

UV-Vis reflection spectra of NAA with different time of anodization, all recorded at nearly normal incidence, are shown in Fig. 3 (a) and (b). The significant inter-band transition at around 1.5 eV for aluminum leads to a local minimum at the wavelength around 825 nm in all the reflection spectra [Tsao et al., 2012]. The oscillations or the fringe pattern in the spectra can be explained by the phenomenon of Fabry-Perot interference. It can be assumed that metal-alumina and the alumina-air interfaces both are at least partly reflective [Zhang et al., 2006]. This interference pattern was used to determine the thickness of the NAA membrane, knowing both the refractive index and the angle of incidence and the results are presented in Fig. 2(c).
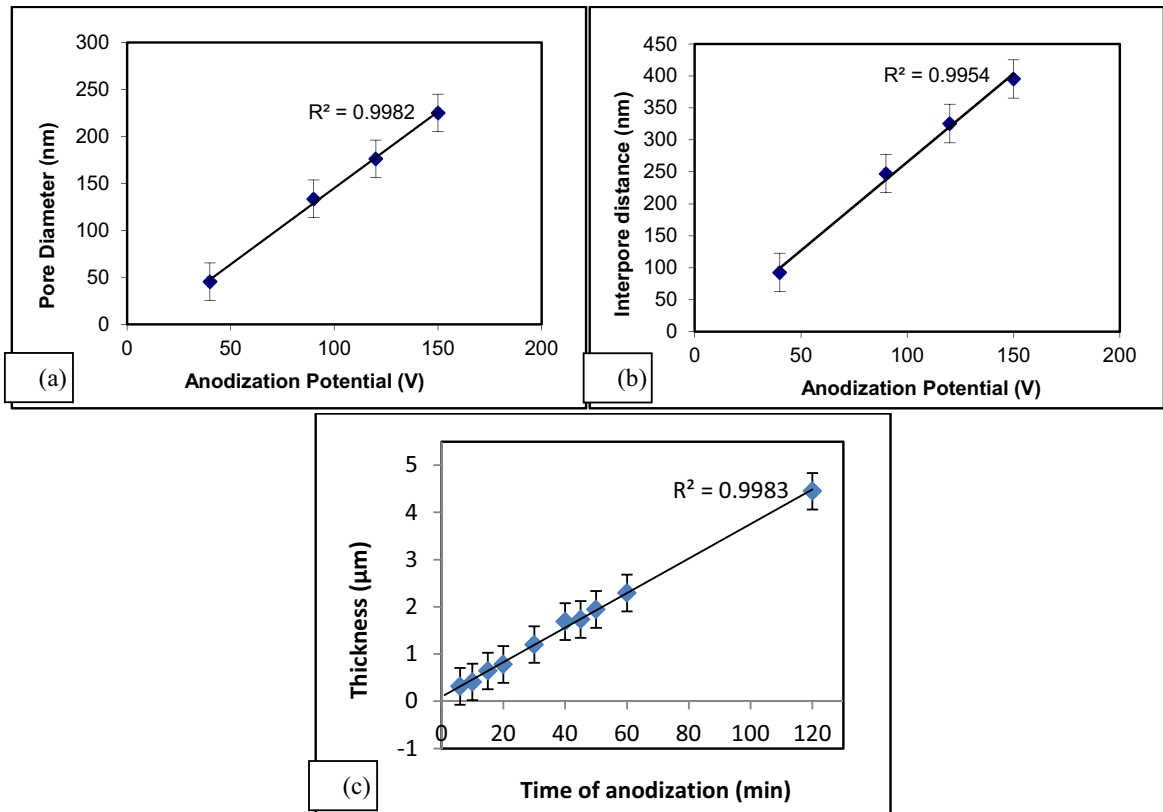
Fig. 2. Graphs showing the dependence of pore diameter (a) and interpore distance (b) on applied voltage for NAA prepared in oxalic and phosphoric acid solutions. (c) Graph showing the dependence of pore length of nanopores of NAA on anodization time under a constant anodization potential of 40 V.
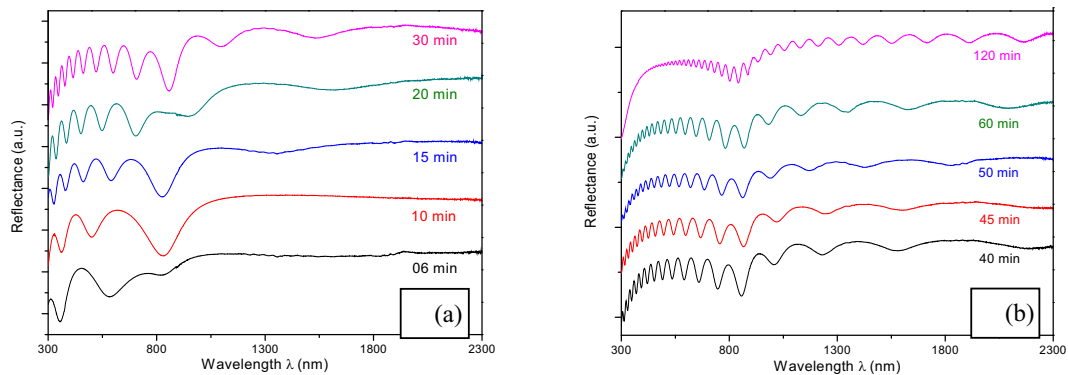

Fig. 3. (a) and (b) Fabry-Perot interference spectrum of NAA obtained at various durations at near normal incidence of the incident light

The refractive index of pure alumina was taken to be 1.7 [Zhang et al., 2006]. In our case the alumina is porous and hence the effective dielectric coefficient was calculated using Maxwell-Garnett theory considering the porosity of the samples. The anodization potential was maintained constant during all these sample preparation as the growth rate of the nanopores depends on the applied voltage also. With increasing time period the lengths of nanopores or the thicknesses of the NAA membranes were also increasing. The intensity of the interference signal was generally high. Initially at smaller values of anodization time there are very few peaks in the Fabry-Perot interference pattern of the optical spectra. With the increase in time the number of peaks started increasing i.e., the number of peaks was

found to depend on the pore lengths of the NAA membrane. As the anodization time increased from 6 minutes to 120 minutes, the number of peaks in the optical spectra started increasing from 3 to 40 (Fig. 4(a)). For NAAs prepared with higher thicknesses it became difficult to interpret the interference spectra and hence no information could be obtained from such spectra. Hence the study was conducted with samples anodized up to 2 hours.

No significant oscillations were observed when the synthesis time was less than 3 minutes. As the time increased to 10 minutes, the number of oscillations started growing with a slight increase in the amplitude of the oscillations in the visible region. The trend continued and the peaks became indiscernible in the visible region for higher anodization times. Initially the oscillations or the fringes are observed in the low wavelength region in the spectrum and the waves gradually moved to the near infrared region by 120 minutes. This red shift of fringes with time was also accompanied with a slow initial rise and then fall in the amplitudes of the oscillations at higher thicknesses. The peak or fringe height also varied with time. It was observed that for 20 minutes NAA the peak height was maximum of 13 nm and then started declining (Fig. 4(a)). The height of peaks can be an important parameter in sensing applications where NAA membranes will be used as a substrate. The optimized thickness of the NAA with appropriate number of peaks and peak height will be helpful in detecting any change in the refractive index of the substrate with and without the sensing medium. This change in refractive index can be seen as a shift in the wavelength of oscillations which in turn will be useful in sensing of any foreign matter on the substrate.
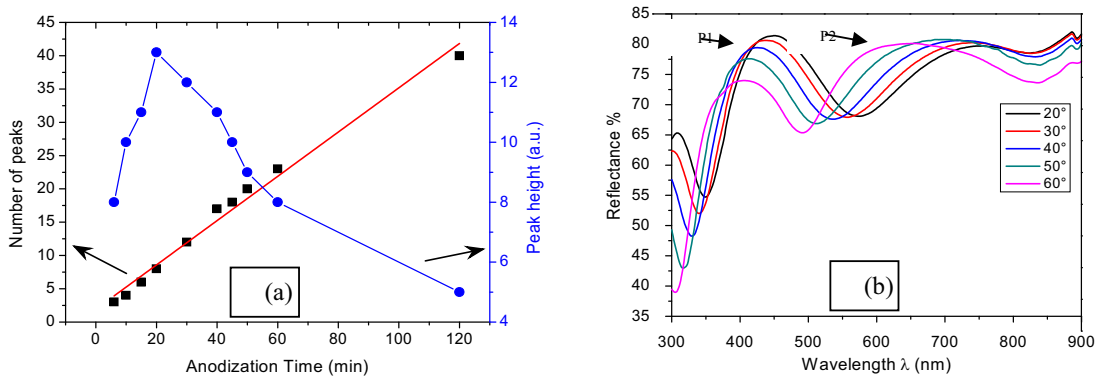

Fig. 4. (a) A graph showing the linear dependence of number of peaks on time of anodization (b) UV-Vis reflectance spectra of the NAA membranes anodized for 6 min recorded using white light incident from different incident angles starting from 20° to 60°
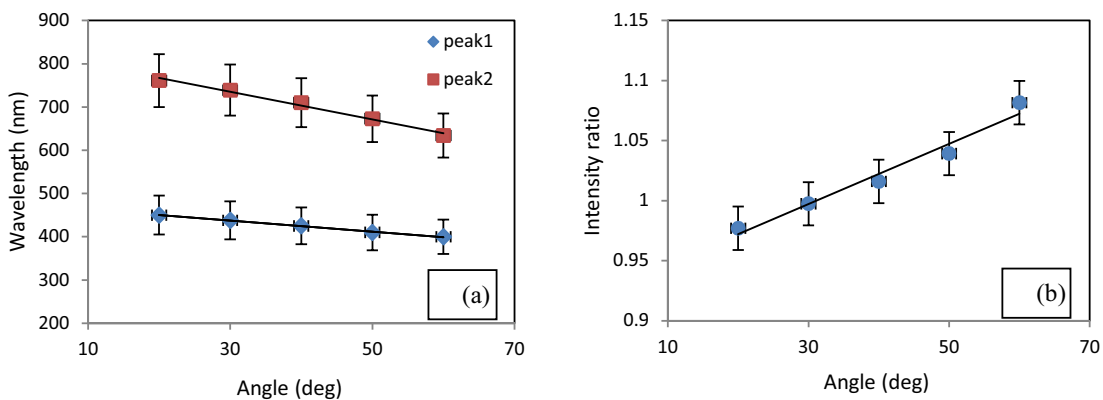

Fig. 5. (a) Graph showing shift of peak position with angle of incidence, (b) intensity ratio of peak 2 (P2) to peak 1 (P1)

The iridescence properties of NAA membranes were studied by varying the angle of incidence of the incident light from near zero to 60°. There is a change in color of the NAA membranes prepared with the anodization time

from 1 minute to 2 minutes. The color changes with the angle of incidence of the light used to view the membranes as shown in Fig. 4 (b). The peaks P1 and P2, as shown in the figure, shift their position towards the blue end of the spectra with the increase in angle. Though both the peaks show the blue shift, their rate of change was found to be different (Fig. 5(a)). With increasing angle it was observed that the intensity of P1 decreased and that of P2 increased. The ratio of intensities of P2 to P1 is plotted in Fig. 5(b). It was seen that with the blue shift of both the peaks with respect to the incident angle, P1 intensity was reduced and P2 intensity increased, shifting the maximum intensity from blue to green region of the spectra confirming the iridescent properties of the prepared NAA membranes. Efforts are on to explore the applicability of NAA membranes by varying their pore properties and combining with the metal monolayer deposition for varying the optical color and enhancing the interferometric properties to be used in sensing applications in the field of biotechnology and medicine.

4. Conclusions

NAA membranes with highly ordered nanopore arrays were prepared with controlled geometrical features. The pore properties of NAA, such as pore diameters, interpore distances and pore lengths were determined for various values of anodization potential and also with different duration keeping the potential constant. The optical interferometric properties of NAA using UV-Vis-NIR spectroscopy were investigated. The effective optical thickness of NAA membranes were calculated using the reflectance spectra. It was observed that the maxima of the reflected wavelengths showed intensity variation with respect to the angle of incidence. Such NAA membranes can be used as substrates for applications such as decoration, display, anti-counterfeiting technology and sensitive and selective bio-sensing applications etc.

Acknowledgements

References

Choudhari, K.S., Jidesh, P., Sudheendra, P., Kulkarni, S.D., 2013. Quantification and Morphology Studies of Nanoporous Alumina Membranes: A New Algorithm for Digital Image Processing. Microscopy and Microanalysis 19, 1061–1072.

Gao, X., Liu, L., Birajdar, B., Ziese, M., Lee, W., Alexe, M., Hesse, D., 2009. High-Density Periodically Ordered Magnetic Cobalt Ferrite Nanodot Arrays by Template-Assisted Pulsed Laser Deposition. Advanced Functional Materials 19, 3450-3455.

Sudheendra, P., Surendranathan, A.O., Udayashankar, N.K., Choudhari K.S., 2012a. Titanium-Aluminium intermetallic thin films preparation by DC sputtering and their characterization. International Journal of Mechanical Engineering 2, 12-17.

Sudheendra, P., Surendranathan, A.O., Udayashankar, N.K., 2012b. Titanium-Aluminium thin films preparation by oblique angle sputtering and their characterization. International Journal of Engineering Research and Technology 1, 1-5.

Biswas, K., Qin, Y., DaSilva, M., Reifenberger, R., Sands, T., 2007. Electrical properties of individual gold nanowires arrayed in a porous anodic alumina template. Physica Status Solidi (A) 204, 3152-3158.

Liu, Z., Chang, P. Chang, C., Galaktionov, E., Bergmann, G., Lu, J.G., 2008. Shape Anisotropy and Magnetization Modulation in Hexagonal Cobalt Nanowires. Advanced Functional Materials 18, 1573-1578.

Sklar, G.P., Paramguru, K., Misra, M., LaCombe, J.C., 2005. Pulsed electrodeposition into AAO templates for CVD growth of carbon nanotubes arrays. Nanotechnology 16, 1265-1271.

Belwalkar, A., Grasing, E., Geertruyden, W.V., Huang, Z., Misiolek, W.Z., 2008. Effect of processing parameters on pore structure and thickness of anodic aluminum oxide (AAO) tubular membranes. Journal of Membrane Science 319, 192-198.

Choudhari, K.S., Jidesh, P., Udayashankar, N.K., 2012a. Fabrication of Nanoporous Alumina and Their Structural Characteristics Study Using SEM Image Processing and Analysis. Synthesis and Reactivity in Inorganic, Metal-Organic and Nano-Metal Chemistry 42, 369-375.

Xu, Q., Yang, Y., Liu, L., Gu, J., Liu, J., Li, Z., Sun, H., 2011. Synthesis and Optical Properties of Iridescent Porous Anodic Alumina Thin Films. Journal of the Electrochemical Society 159, C25-C28.

Wang, X., Zhang, D., Zhang, H., Ma, Y., Jiang, J.Z., 2011. Tuning color by pore depth of metal-coated porous alumina. Nanotechnology 22, 305306.

Kumeria, T., Rahman, M.M., Santos, A., Ferre-Borrull, J., Marsal, L.F., Losic, D., 2014. Structural and Optical Nanoengineering of Nanoporous Anodic Alumina Rugate Filters for Real-Time and Label-Free Biosensing Applications. Analytical Chemistry 86, 1837-1844.

Kumeria, T., Santos, A., Losic, D., 2013. Ultrasensitive Nanoporous Interferometric Sensor for Label-Free Detection of Gold(III) Ions. Applied Materials & Interfaces 5, 11783-11790.

Choudhari, K.S., Sudheendra, P., Udayashankar, N.K., 2012b. Fabrication and high-temperature structural characterization study of porous anodic alumina membranes. Journal of Porous Materials 19, 1053-1062.

Li, A.P., Muller, F., Birner, A., Nielsch, K., Gosele, U., 1998. Hexagonal pore arrays with a 50–420 nm interpore distance formed by self-organization in anodic alumina. Journal of Applied Physics 84, 6023-6026.

Tsao, Y., Sondergaard, T., Skovsen, E., Gurevich, L., Pedersen, K., Pedersen, T.G., 2012. Pore size dependence of diffuse light scattering from anodized aluminum solar cell backside reflectors. Optics Express 21, A84-A95.

Zhang, D., Zhang, H., He, Y., 2006. In-Situ Thickness Measurement of Porous Alumina by Atomic Force Microscopy and the Reflectance Wavelength Measurement From 400–1000 nm. Microscopy Research and Technique 69, 267-270.